

Propagation of random excitations in the polar representation of strongly nonlinear four-wave systems of turbulence

Wonjung Lee *

Research Center for Mathematics, Beijing Normal University at Zhuhai 519087, China
and Department of Mathematical Sciences, United International College (BNU-HKBU), Zhuhai 519087, China

 (Received 19 May 2023; accepted 16 November 2023; published 18 December 2023)

The present work is concerned with the uncertainty propagation of the wave turbulent system. In particular, we study the temporal development and long-term behavior of the probability with respect to the amplitude and phase of complex-valued waves constituting the generic four-wave system of turbulence. Our approach to approximating the target distribution function is via the three steps: (i) to grasp the physical process described by the true turbulence model as random process, (ii) to determine the stochastic differential equation whose solution exhibits statistically similar behavior with the underlying turbulent signal, and (iii) to solve the corresponding Kolmogorov forward equation. Our implementation of the methodology is distinguished by employing a number of simplified stochastic models and applying one of them in the adaptive fashion which varies subject to the different parameter regime of the true dynamical system model. Accordingly, we become able to demonstrate the effectiveness of this reduced-order modeling framework for the analysis of the turbulent system characterized by not only weak but strong interactions among the nonlinear waves. We numerically corroborate our theoretical predictions in the context of the generalized Majda-McLaughlin-Tabak wave turbulence prototype.

DOI: [10.1103/PhysRevE.108.064126](https://doi.org/10.1103/PhysRevE.108.064126)

I. INTRODUCTION

A. Overview

A group of nonlinearly interacting waves arises in numerous branches of physics. Examples include surface waves, capillary waves, internal waves, waves on liquid hydrogen, Alfvén and Langmuir waves in plasmas, and turbulence in nonlinear optics [1–3]. Such dynamical systems often absorb and dissipate energy at vastly different spatial and temporal scales, giving rise to the emergence of an intermediate range between the well-separated forcing and dissipation areas in the wave-number domain. In this extensive inertial range, due to the nearly conservative characteristics of the dynamics, Hamiltonian formulation is apt for a mathematical description of the relevant physical phenomena. This means that the evolution equation of the complex-valued variable a_k for the wave turbulence can be written as the canonical equation

$$i\partial_t a_k = \frac{\delta H}{\delta a_k^*}, \quad (1)$$

where k is the Fourier index, H is Hamiltonian, and the upper * signifies complex conjugation.

In particular, our treatment in this work will focus on the Hamiltonian of the form

$$\begin{aligned} H &= \sum_k \chi \omega_k |a_k|^2 + \frac{1}{2} \sum_{k_{1234}} W_{34}^{12} \delta_{34}^{12} a_1 a_2 a_3^* a_4^* \\ &= \chi H_2 + H_4, \end{aligned} \quad (2)$$

where $k_{1234} = k_1, k_2, k_3, k_4$ and a_j is shorthand notation of a_{k_j} for $j = 1, 2, 3, 4$. Here $W_{34}^{12} (> 0)$ is the control parameter

for the four-wave interactions, and δ_{34}^{12} equals 1 if $k_1 + k_2 - k_3 - k_4 = 0$ and zero otherwise. The coefficient χ assumes the binary value of unity or zero. For the case when $\chi = 1$, one can read from the corresponding Hamilton's equation of motion,

$$i\partial_t a_k = \chi \omega_k a_k + \sum_{k_{123}} W_{3k}^{12} \delta_{3k}^{12} a_1 a_2 a_3^*, \quad (3)$$

that the physical quantity represented by the canonical variable a_k is the nonlinear wave in possession of the linear dispersion relation ω_k . The nonlinear Schrödinger equation

$$i\partial_t u = -\partial_x^2 u + |u|^2 u \quad (4)$$

in one space dimension exemplifies such a class of dynamical systems: the substitution of $u(x, t) = \sum_k a_k(t) e^{ikx}$ into (4) leads to the dynamics (3) instantiated by $\omega_k = |k|^2$ and $W_{34}^{12} = 1$.

It is indeed physically fruitful to extend dynamic regimes to more general nonlinear regimes. For the four-wave system of (2), this can be achieved by considering the case of $\chi = 0$. The consequence is that the scope of nature phenomena mimicked by the model equation (3) is broader than the ones arising from a set of dispersive waves. This is because for the case when $\chi = 0$ and no linear dispersion exists, the system has a certain similarity with Clebsch formulation of the Euler equation in the ideal hydrodynamics [4]. Due to the capability of encompassing many nonlinear dynamical system models and as a result creating a variety of turbulent signals with distinctive characteristics, our study of turbulence phenomena within the context of (2) ensures a considerable degree of generality.

Turbulence models such as (3) tend to exhibit highly disordered and unorganized system behavior [1–3]. Rather

*wonjunglee@bnu.edu.cn

than unveiling and elucidating the superfluous details of the trajectories of the dynamical processes, our explanation of the relevant phenomena is by virtue of the concepts from probability theory. Now, taking this probabilistic perspective, our main duty has become the quantification of the propagating uncertainty induced by the initial randomness of the deterministic model system (1). Though the ultimate goal is to characterize the full joint probability distribution for the entire system variables, our description in the present work is restricted to one mode and we focus on determining the uncertainties associated with the single variable a_k only. Later, we will additionally care the cross-correlations among the modes and complete the whole picture by interconnecting and interweaving altogether the element-wise information about possibly very different probabilistic characters of the individual members.

For wave systems, we are interested in the complex-valued waves and their polar representations. The primary reason is that many observables in the real-world wave phenomena are directly related to the complex-valued wave expressions in the rectangular and polar coordinates, and one can capture the statistical properties of physically interesting quantities from those of the wave amplitude and phase angle [2,3]. Furthermore, the thorough investigation of the complex-valued random variable must include the discussion of the uncertainties with reference to the corresponding polar components. Let $s_k = |a_k|^2$ and $\phi_k = \arg(a_k)$ be the amplitude and phase of the wave-profile $a_k = \sqrt{s_k}e^{i\phi_k}$, then we are led by the above arguments to study the joint and marginal distribution functions of s_k and ϕ_k . One way to do this is through deriving a differential equation which governs the time evolution of the relevant probability and solving it. In this research direction, one previous result is the PDE

$$\partial_t P_k(t, s) = \partial_s (2\gamma_k s P_k + 2\eta_k s \partial_s P_k) \quad (5)$$

for which $\Pr[s < s_k(t) \leq s + ds] = P_k(t, s)ds$ and $\Pr[\dots]$ means the probability of the event in the bracket occurring. Here the coefficients γ_k and η_k are given in terms of the probability of other modes via the second-order moments. It is demonstrated in a body of work [5–7] that the random fluctuations in the wave amplitude are approximately distributed according to the solution of Eq. (5) for the case when $\chi = 1$ and $H_4/H_2 \ll 1$ (the designated system is one main concern in the classical wave turbulence theory [2,3], and hereafter will be referred to as the weak turbulence).

B. The goal and methodology

This successful formulation of the transparent and comprehensible framework for the study of wave amplitude in case of weak turbulence creates a clear motivation for the extension of the existing development and provides a real momentum for us to undertake the current research of addressing (i) both the amplitude and phase variables and (ii) both the weakly and strongly nonlinear dynamical systems. Specifically, our purpose is to shed further light on the pioneering achievement for the weak turbulence through the derivation and analysis of some analogs of the PDE (5) so that one can determine the temporal change and the long-term behavior of the probability of s_k and ϕ_k with regard to the dynamic variable a_k as the

solution of the four-wave system (2) and (3). Importantly, our discussion will not only treat the weak turbulence, i.e., the system with $\chi = 1$ and $H_4/H_2 \ll 1$, but also cover two representative cases of the strong nonlinearities: (i) when $\chi = 1$ and H_4/H_2 is not a small number and (ii) when $\chi = 0$.

To carry out the program, we employ a number of reduced-order models for the purpose of approximating the uncertainties in the polar variables of the turbulent signal generated from the Hamiltonian system involving the four-wave interactions. Specifically, we proceed by carefully choosing the stochastic differential equation (SDE) model which can capture the key features of the true signal a_k at the statistical level and by studying the Kolmogorov forward equation (KFE) which governs the probability distribution arising from the polar representation of the stochastic process model. We also perform the numerical study verifying that for the Majda-McLaughlin-Tabak prototypical wave turbulence system in thermal equilibrium, the suggested models are capable of describing the probability of amplitude and phase of the true underlying signal to a reasonable accuracy.

C. Organization of the paper

The exposition of our work closely follows the standard way of utilizing simplified models for the analysis of the complex dynamical system and demonstrating the effectiveness of the methodology. Accordingly, the remainder of this paper is arranged in the order of (i) proposing the reduced-order models in connection with the wave turbulence model (Sec. II), (ii) analyzing the approximate models so as to make the theoretical predictions for the underlying turbulent signal (Secs. III and IV), and (iii) showing their good agreement with the results from the direct numerical simulation of the true complex model (Sec. V). To be more precise, in Sec. II, we introduce two Markov process models and one non-Markov process model. Those are the coarse-grained equations of motion for the original dynamical system model (3). Subsequently, we devote Sec. III to the discussion of Markov models and Sec. IV to that of non-Markov model. In Sec. V, we numerically demonstrate the outperformance of the non-Markov process model over the other Markov process models in approximating the probabilities related to the shortwave turbulent signal coming from the strongly nonlinear four-wave dynamics. The paper is then concluded with giving some remarks in Sec. VI.

II. REDUCED-ORDER MODELS FOR THE FOUR-WAVE SYSTEM

We begin the presentation of the reduced-order models with the climatological stochastic model or CSM for short. The equation of motion is given by

$$\text{(CSM)} \quad \hat{a}_k = -(i\chi\omega_k + \gamma)\hat{a}_k + \sqrt{2\eta}\dot{W}_k, \quad (6)$$

(throughout this paper, we let \hat{a}_k represent a statistical approximation of the true signal a_k) where the overdot signifies the time differentiation and \dot{W}_k denotes the complex-valued white noise. Here γ and η are the positive tunable parameters, controlling the strength of the linear dissipation and white

noise forcing. Rewriting (3) as

$$\dot{a}_k = -i\chi\omega_k a_k + N_k, \quad (7)$$

one can recognize that CSM is the result from the approximation

$$\begin{aligned} N_k &\equiv -i \sum_{k_{123}} W_{3k}^{12} \delta_{3k}^{12} a_1 a_2 a_3^* \\ &\simeq -\gamma a_k + \sqrt{2\eta} \dot{W}_k, \end{aligned} \quad (8)$$

i.e., the nonlinear interactions are replaced by the linear dissipation and white noise forcing.

Such a coarse-graining technique is often adopted for the modeling of Brownian motion, and experience has shown that the resulting SDE can ensure a reasonable accuracy in reproducing the statistical properties of the true signal provided that $a_k(t)$ is a slowly varying dynamic process. This condition holds for the weak turbulence system which indicates a sharp timescale separation between the typical motions of a_k and N_k . However, stepping outside of the weak turbulence (that is, for the case when $\chi = 1$ and the value of H_4/H_2 is not so small, or for the case when $\chi = 0$), a formal application of this conventional scheme would be highly inappropriate for the phenomenological description of the true turbulent signal. This significant limitation of CSM in accounting for strong wave turbulence provides us with the impetus for the development of new reduced-order models.

In a body of work [8–11], the author has designed a number of simplified reductions of the four-wave Hamiltonian system (2) and (3) which lies beyond the weak nonlinearity regime, and here two of them are introduced. The mean stochastic model (MSM) takes the form

$$\text{(MSM)} \quad \dot{\hat{a}}_k = -(i\Omega_k + \gamma)\hat{a}_k + \sqrt{2\eta} \dot{W}_k, \quad (9)$$

and the difference from CSM occurs in the oscillation parameter

$$\Omega_k \equiv \chi\omega_k + \sum_{k'} (W_{k'k}^{k'k} + W_{k'k}^{kk'}) \langle |a_{k'}|^2 \rangle. \quad (10)$$

Here and after, the angle bracket denotes the ensemble average against the stationary distribution. The autoregressive model (ARM) is the non-Markovian process model given by

$$\begin{aligned} \text{(ARM)} \quad \dot{\hat{a}}_k &= -(i\Omega_k + \gamma)\hat{a}_k + \sqrt{2\eta} \dot{W}_k \\ &- \int_0^t d\tau \mathcal{A} e^{-(i\Omega_k + \nu)(t-\tau)} \hat{a}_k(\tau) + \tilde{R}, \end{aligned} \quad (11)$$

where \tilde{R} is the Ornstein-Uhlenbeck process (OUP) satisfying $\langle \tilde{R}(t)\tilde{R}(0)^* \rangle / \langle |\hat{a}_k|^2 \rangle = \mathcal{A} e^{-(i\Omega_k + \nu)t}$. Here \mathcal{A} is positive real and $\nu = \nu_r + i\nu_i$ is a complex number with positive real part. Those are the adjustable parameters and respectively related with the magnitude and decorrelation time of the nonwhite noise \tilde{R} .

The adaptive use of the presented reduced-order models in mimicking the true underlying signal should refer to the conditions on the strength of nonlinearity of the wave turbulence system (3) and on the wave number k of the dynamic process a_k , which can be found in Table I.

Below we give a brief outline of the systematic derivation of MSM and ARM. It is worth emphasizing that our

TABLE I. The various reduced-order models for the true turbulent signal a_k and their validity regime for an accurate description of the probabilistic character of the Hamiltonian system (2).

Model	Time-lag	χ	H_4	Wavelength(k)
CSM	Markov	1	Weak	All
MSM	Markov	0,1	Moderate/strong	All/longwave (small)
ARM	Non-Markov	0,1	Strong	Shortwave (large)

construction of these coarse-grained equations of motion is made through a detailed analysis of the nonlinearities denoted by N_k . Concretely, we divide the set of nonlinear interactions into distinct classes and verify their different roles and characteristic timescales in affecting the target system variable a_k .

Above all, we perform the decomposition of the nonlinearity

$$N_k = T_k + N_k^{\text{eff}}, \quad (12a)$$

$$\begin{aligned} T_k &\equiv -i \sum_{k_{123}, k_{12}=k} W_{3k}^{12} \delta_{3k}^{12} a_1 a_2 a_3^* \\ &= -i \left[\sum_{k'} (W_{k'k}^{k'k} + W_{k'k}^{kk'}) |a_{k'}|^2 \right] a_k, \end{aligned} \quad (12b)$$

$$N_k^{\text{eff}} \equiv -i \sum_{k_{123}, k_{12} \neq k} W_{3k}^{12} \delta_{3k}^{12} a_1 a_2 a_3^*. \quad (12c)$$

Here T_k singles out the trivial resonances, for which $k_{12} = k$ means $k_1 = k$ or $k_2 = k$. It turns out that the corresponding terms essentially do not contribute to the energy-momentum exchange between the modes but their collective effect plays the crucial role in determining the effective dispersion relation of a_k by Ω_k in (10). The mean-field equation

$$\dot{a}_k \doteq -i\Omega_k a_k + N_k^{\text{eff}} \quad (13)$$

emerges as a consequence of statistically averaging the coefficient of a_k in (12b), and one can make use of (13) for a more realistic description of the dynamical and statistical pictures exhibited by the genuine dynamics of (3) and (7) [12]. Note N_k^{eff} operates as the nonlinear interactions in (13) and thus is called the effective nonlinearity. By performing the approximation analogous to (8), i.e., applying

$$N_k^{\text{eff}} \simeq -\gamma a_k + \sqrt{2\eta} \dot{W}_k \quad (14)$$

to (13), we obtain MSM.

In cases where MSM shows a poor performance, the modeling of (14) must be revised. To do this, we attempt the further decomposition of the effective nonlinearity

$$N_k^{\text{eff}} = A_k + N_k^{\text{resid}}, \quad (15a)$$

$$A_k \equiv -i \sum_{k_{123}, k_{12} \neq k, |\Omega_{3k}^{12}| \doteq 0} W_{3k}^{12} \delta_{3k}^{12} a_1 a_2 a_3^*, \quad (15b)$$

$$N_k^{\text{resid}} \equiv -i \sum_{k_{123}, k_{12} \neq k, |\Omega_{3k}^{12}| > 0} W_{3k}^{12} \delta_{3k}^{12} a_1 a_2 a_3^*, \quad (15c)$$

where $\Omega_{3k}^{12} = \Omega_{k_1} + \Omega_{k_2} - \Omega_{k_3} - \Omega_k$. As for (15b), we gather the terms being resonant with a_k in the nontrivial ($k \neq k_1, k_2$) manner to form the auxiliary variable A_k so that this

macrovariable has a strong interaction with the target system variable. By contrast, the interaction between a_k and the residual nonlinearities denoted by N_k^{resid} is insignificant on the long-term basis. We build this knowledge into the following approximations:

$$A_k \simeq - \int_0^t d\tau \tilde{\Gamma}(t-\tau) a_k(\tau) + \tilde{R}(t), \quad (16a)$$

$$N_k^{\text{resid}} \simeq -\gamma a_k + \sqrt{2\eta} \dot{W}_k, \quad (16b)$$

which reflect two distinct ways of influencing of A_k and N_k^{resid} on a_k through forcing and dissipation in the non-Markovian and Markovian fashion. Here the memory kernel $\tilde{\Gamma}$ is responsible for the time-lag dissipation. The combination of (13), (15a), and (16) yields a regression model with memory. Particularly, from choosing the damping coefficient $\tilde{\Gamma}$ by the exponential function and identifying \tilde{R} by the OUP, this non-Markov process model reduces to ARM (11).

Finally, we endow the heuristic development of ARM sketched in the preceding paragraph with a degree of theoretical justification [10,11]. To this end, we derive a bivariate diffusion model by making use of the Mori-Zwanzig projection formalism to achieve the exact rearrangement of the Liouville equation governing the pair of variables (a_k, A_k) and then by performing some reasonable approximations for the coefficients in the resulting generalized Langevin equation. Marginalizing the auxiliary variable A_k in this two-dimensional vector SDE leads to ARM, and this alternative but more rigorous development of ARM gives further depth to the demonstration about the effectiveness of the modeling of (16) based on our intuition and strengthens the plausibility of ARM.

In the next two sections, we perform the theoretical analysis of the simplified stochastic models and apply the gained knowledge for the prediction of the probabilities with regard to the true turbulent signal a_k .

III. TURBULENT SIGNAL MODELED BY A MARKOV PROCESS

Let us consider CSM (6) and MSM (9). Introducing the variable $z_k(t) = e^{i\omega_k t} \hat{a}_k(t)$ in case of CSM and $z_k(t) = e^{i\Omega_k t} \hat{a}_k(t)$ in case of MSM, both linear Markov models are transformed into the common form of

$$(\text{CSM/MSM}) \quad \dot{z} = -\gamma z + \sqrt{2\eta} \dot{W}_z, \quad (17)$$

where the subindex k is dropped for the sake of notational simplicity. Here the parameters γ and η are positive reals and possibly depend on time, and \dot{W}_z is complex-valued white noise.

We first devote Secs. III A, III B, and III C to the study of the OUP in (17). In particular, we determine the probability distributions for the processes of z , $s = |z|^2$, $\theta = \arg(z)$, and their long-time behavior. We proceed by addressing the case when the random variable z at $t = 0$ is distributed by Gaussian (Secs. III A and III B) and then investigating a more generic situation where the initial probability $P(t = 0, z)$ is away from the Gaussian distribution (Sec. III C). Next, in Sec. III D, we discuss the utility and limitations of the SDE-based approach for the analysis of real-world turbulent signals.

A. Complex-valued Gaussian process

A complex-valued random variable $z = x + iy$ is referred to as Gaussian provided that both real and imaginary parts are independently distributed according to Gaussian distribution and are in possession of the same variance. That is, by $z \sim \mathcal{N}(\mu = \mu_x + i\mu_y, \Sigma = 1/\Lambda)$ we mean $x \sim \mathcal{N}(\mu_x, \Sigma/2)$ and $y \sim \mathcal{N}(\mu_y, \Sigma/2)$. Recall $P(x) = \exp[-(x - \mu_x)^2/\Sigma]/\sqrt{\pi\Sigma}$ where $P(\cdot)$ denotes the probability density function, then $P(x, y) = P(x)P(y)$ in two-dimensional space can be represented as

$$P(z) = \frac{\Lambda}{\pi} e^{-\Lambda|z-\mu|^2} \quad (18)$$

using the complex number notation. Here $\Lambda = 1/\Sigma$ is the reciprocal of variance, called the precision.

We now let z_t be a time series of random variable having t as continuous parameter. When this stochastic process satisfies the linear equation in (17), the Gaussian character of the initial randomness will be preserved in the course of time. Such dynamics forms one example of Gaussian process, for which the evolving probability is determined by the mean and variance. Especially, Eq. (17) admits the solution

$$\begin{aligned} z_t &\sim \mathcal{N}(\mu_t, \Sigma_t = 1/\Lambda_t), \\ \mu_t &= \Phi_t \mu_0, \quad \Phi_t = e^{-\int_0^t d\tau \gamma(\tau)} \\ \Sigma_t &= |\Phi_t|^2 \left[\Sigma_0 + \int_0^t d\tau \frac{2\eta(\tau)}{|\Phi_t|^2} \right] \\ &\equiv |\Phi_t|^2 \Sigma_0 + \Sigma'_t, \end{aligned} \quad (19)$$

where Φ_t is the integrating factor satisfying $\dot{\Phi}_t = -\gamma\Phi_t$ and $\Phi_0 = 1$. The Gaussian function (18) parameterized by the coefficients in (19) solves the KFE corresponding to the SDE in (17). Note that $W_z = (B_x + iB_y)/\sqrt{2}$ is a complex-valued Brownian motion with B_X denoting real-valued Brownian motion, mutually independent for different X . Then writing (17) as

$$\begin{aligned} dx &= -\gamma x dt + \sqrt{\eta} dB_x, \\ dy &= -\gamma y dt + \sqrt{\eta} dB_y, \end{aligned} \quad (20)$$

the relevant PDE reads as

$$\partial_t P(t, x, y) = \partial_x (\gamma x P + \frac{\eta}{2} \partial_x P) + \partial_y (\gamma y P + \frac{\eta}{2} \partial_y P) \quad (21)$$

in rectangular coordinates.

B. From rectangular to polar coordinates

Here we move from rectangular to polar representation of the statistical model (17).

1. Differential equations governing the evolution of distribution functions in polar coordinates

Let $z = \sqrt{s} e^{i\theta}$ then the recast of (17) in polar coordinates is given by the set of Itô differential

equations

$$ds = (-2\gamma s + 2\eta)dt + \sqrt{4\eta s} dB_s, \quad (22)$$

$$d\theta = \sqrt{\frac{\eta}{s}} dB_\theta, \quad (23)$$

and the corresponding KFE

$$\partial_t P(t, s, \theta) = \partial_s(2\gamma s P + 2\eta s \partial_s P) + \frac{\eta}{2s} \partial_\theta^2 P \quad (24)$$

governs the joint probability for the polar variables.

Below we address the problem of finding the closed equations for the marginal distributions: $P(t, s) = \int d\theta P(t, s, \theta)$ and $P(t, \theta) = \int ds P(t, s, \theta)$. The former equation regarding the progress of the amplitude is readily found by integrating the differential equation in (24) over the phase variable. Using the periodic boundary condition, the task yields

$$\partial_t P(t, s) = \partial_s(2\gamma s P + 2\eta s \partial_s P). \quad (25)$$

Note that the Markovian form of (25) is fully consistent because, in view of (22), the dynamics of s is not affected by θ . In effect, Eq. (25) is the KFE corresponding to the SDE (22) for the amplitude process.

By contrast, the latter equation governing the phase variable cannot be obtained simply by marginalizing the KFE (24) for the joint distribution. The failure is due to the dependence of θ on s , as can be seen from (23). At this point, we conduct the projection of the full joint distribution onto the space of marginal distribution in order to rearrange the PDE in (24) and to produce the desired output [13]. The resulting integrodifferential equation is given by

$$\begin{aligned} \partial_t P(t, \theta) &= \int ds L_1 \varphi_\infty(s) P(t, \theta) \\ &+ \int ds L_1 \int_0^t d\tau e^{(t-\tau)(1-\mathcal{P})L} \\ &\times (1 - \mathcal{P}) L_1 \varphi_\infty(s) P(\tau, \theta) \\ &+ \int ds L_1 e^{t(1-\mathcal{P})L} (1 - \mathcal{P}) P(t = 0, s, \theta), \end{aligned} \quad (26)$$

where $L = L_0 + L_1$ is the forward operator with $L_0 = \partial_s(2\gamma s + 2\eta s \partial_s)$ and $L_1 = \frac{\eta}{2s} \partial_\theta^2$ and \mathcal{P} represents the projection onto the resolved mode defined by $\mathcal{P}f(s, \theta) = \varphi_\infty(s) \int ds f(s, \theta)$ with some invariant measure φ_∞ (see Sec. III C 3 for a discussion of the choice). Note that Eq. (26) is derived under the assumption that the associated parameters are constants; the presentation of such form here is mostly for simplicity of notation, and it is straightforward to formulate the case of otherwise.

2. Particular solution of the differential equations for polar variables

Here we would like to quantify the uncertainty with respect to the polar variables (s, θ) propagated by the coupled SDEs in (22) and (23) and further to determine the marginal distribution of each component. This can be achieved by solving the governing equations of (24)–(26). In doing so, rather than implementing some well-known numerical schemes, we make

a clever use of the fact that this set of nonlinear (and even non-Markov) problems is nothing but a linear Markov problem in disguise. Specifically, our key idea for the resolution is to reverse the construction argument used for deriving the sequence of differential equations; (i) one can solve (25) and (26) by seeking the solution of the KFE (24) for the double variables and integrating out the irrelevant one; (ii) Eqs. (21) and (24) are the distinct representations of the same content, implying that solving one amounts to solving the other.

First, we find one class of solution to the PDE (24) by making the change of variable. That is, by substituting $z = \sqrt{s}e^{i\theta}$ into (18), we obtain

$$\begin{aligned} P(s, \theta) &= \frac{1}{2} \frac{\Lambda}{\pi} e^{-\Lambda |\sqrt{s}e^{i\theta} - \mu|^2} \\ &= \frac{\Lambda}{2\pi} e^{-\Lambda(s+|\mu|^2 - 2\sqrt{s}|\mu| \cos[\theta - \arg(\mu)])} \end{aligned} \quad (27)$$

as a solution of this KFE for the polar variables. Note the multiplicative factor of Jacobian $\mathcal{J} = 1/2$ resulting from $P(z)dz = [P(z = \sqrt{s}e^{i\theta})\mathcal{J}]dsd\theta = P(s, \theta)dsd\theta$ is taken into account. Here and after, the time index t for the variables $z, s,$ and θ will occasionally be suppressed to keep the notation uncluttered.

Second, we perform the marginalization of the joint distribution (27) to obtain one solution of the differential equations in (25) and (26). They are respectively given by

$$P(s) = \int d\theta P(s, \theta) = \Lambda e^{-\Lambda(s+|\mu|^2)} I_0(2\Lambda\sqrt{s}|\mu|), \quad (28)$$

where

$$I_0(p) \equiv \frac{1}{2\pi} \int_0^{2\pi} d\theta e^{p \cos(\theta)} = \sum_{m=0}^{\infty} (p/2)^{2m} / (m!)^2 \quad (29)$$

is the zeroth modified Bessel function of the first kind, and by

$$\begin{aligned} P(\theta) &= \int ds P(s, \theta) \\ &= \frac{\Lambda}{2\pi} e^{-\Lambda|\mu|^2} F(\Lambda, |\mu| \cos[\theta - \arg(\mu)]), \end{aligned} \quad (30)$$

where

$$\begin{aligned} F(p, q) &\equiv \int_0^{\infty} ds e^{-p(s-2\sqrt{s}q)} \\ &= \frac{1}{p} + 2qe^{pq^2} \sqrt{\frac{\pi}{4p}} [1 + \operatorname{erf}(\sqrt{pq})] \end{aligned} \quad (31)$$

involves the error function (erf). It will help to keep in mind that this machinery of producing the functional form of (27), (28), and (30) for the Gaussian process z in possession of the mean μ and precision Λ will recur repeatedly throughout the remainder of the paper.

3. Choice of the amplitude variable

Before studying the case of non-Gaussian initial condition, we here address the issue of what if the variable $\rho = |z|$ is used in place of $s = |z|^2$ for the polar representation of the stochastic dynamics of (17). In such a case, one needs to deal

with the SDE

$$d\rho = \left(-\gamma\rho + \frac{\eta}{2\rho}\right)dt + \sqrt{\eta}dB_\rho \quad (32)$$

and the corresponding KFE

$$\partial_t P(t, \rho, \theta) = \partial_\rho \left[\left(\gamma\rho - \frac{\eta}{2\rho}\right)P + \frac{\eta}{2} \partial_\rho P \right] + \frac{\eta}{2\rho^2} \partial_\rho^2 P \quad (33)$$

instead of (22) and (24). Note the form of the solution to (33) can also be inherited from the Gaussian function (18) in rectangular coordinates and found by substituting $z = \rho e^{i\theta}$ and caring the Jacobian factor $\mathcal{J} = \rho$ obtained from considering the area element $dxdy = \rho d\rho d\theta$. In this way, one can duplicate basically the same scenario written in terms of probability with what we will provide using the variable s .

C. Transition probabilities

We now discuss the case when the random variable z_0 for the model equation (17) is not necessarily Gaussian. To put it another way, $P(z_0)$ can be different from the form of (18) or, equivalently, $P(t = 0, s, \theta)$ can be different from the form of (27).

1. Rectangular coordinates

Probability theory formalizes the time advance of the random process z_t by combining the initial distribution $P(z_0)$ and the transition probability $P(z_t|z_0)$ via the integral

$$P(z_t) = \int dz_0 P(z_t|z_0)P(z_0), \quad (34)$$

and instructs us that the key quantity for the prediction is the conditional probability distribution of z_t given z_0 .

The process $z_t|z_0$ as a solution of the linear equation (17) possesses the law of Gaussian distribution (intuitively, a point mass can be viewed as Gaussian) characterized by

$$\begin{aligned} z_t|z_0 &\sim \mathcal{N}(\mu'_t, \Sigma'_t = 1/\Lambda'_t), \\ \mu'_t &= \Phi_t z_0, \quad \Phi_t = e^{-\int_0^t d\tau \gamma(\tau)} \\ \Sigma'_t &= |\Phi_t|^2 \int_0^t d\tau \frac{2\eta(\tau)}{|\Phi_\tau|^2}. \end{aligned} \quad (35)$$

Here and after, the prime notation is used to emphasize the quantities in relation to the conditioned variable.

The distribution $P(z_t|z_0)$ is the Gaussian function in (18) with replacing μ and Σ by μ' and Σ' in (35). This expression forms the fundamental solution of the PDE (21) in rectangular coordinates, which starts out at $t = 0$ as a Dirac delta function $P(t = 0, z) = \delta(z - z_0)$. For an arbitrary initial condition $P(z_0)$, the integral representation of the general solution is given by Eq. (34).

2. Polar coordinates

Denoting $P(t = 0, s, \theta)$ by $P(s_0, \theta_0)$, the forward mapping from $P(s_0, \theta_0)$ to $P(s_t, \theta_t)$, and to $P(s_t)$ and $P(\theta_t)$, can be achieved through

$$P(s, \theta) = \int ds_0 d\theta_0 P(s, \theta|s_0, \theta_0)P(s_0, \theta_0), \quad (36)$$

and

$$P(s) = \int ds_0 d\theta_0 P(s|s_0, \theta_0)P(s_0, \theta_0), \quad (37)$$

$$P(\theta) = \int ds_0 d\theta_0 P(\theta|s_0, \theta_0)P(s_0, \theta_0). \quad (38)$$

As for the mapping from $P(s_0)$ to $P(s_t)$ and from $P(\theta_0)$ to $P(\theta_t)$, one can convert (37) and (38) into

$$P(s) = \int ds_0 P(s|s_0)P(s_0), \quad (39)$$

$$P(\theta) = \int d\theta_0 P(\theta|\theta_0)P(\theta_0), \quad (40)$$

together with the kernel functions

$$P(s|s_0) = \int d\theta_0 P(s|s_0, \theta_0)P(\theta_0|s_0), \quad (41)$$

$$P(\theta|\theta_0) = \int ds_0 P(\theta|s_0, \theta_0)P(s_0|\theta_0), \quad (42)$$

by means of the integrals.

Applying the machinery remarked at the end of Sec. III B 2, the transition probabilities for the polar variables are obtained via replacing (μ, Λ) in (27), (28), and (30) by (μ', Λ') in (35) and given by

$$P(s, \theta|s_0, \theta_0) = \frac{\Lambda'}{2\pi} e^{-\Lambda'(s+s_0|\Phi|^2 - 2\sqrt{s s_0}|\Phi| \cos[\theta - \theta_0])}, \quad (43)$$

$$P(s|s_0) = \Lambda' e^{-\Lambda'(s+s_0|\Phi|^2)} I_0(2\Lambda' \sqrt{s s_0} |\Phi|), \quad (44)$$

$$P(\theta|s_0, \theta_0) = \frac{\Lambda'}{2\pi} e^{-\Lambda' s_0 |\Phi|^2} F(\Lambda', \sqrt{s_0} |\Phi| \cos[\theta - \theta_0]). \quad (45)$$

We note that, in case of wave amplitude, Eq. (44) does not involve the variable θ_0 . In case of wave phase, however, one needs to use (42) in order to remove s_0 visible in (45) and to produce the kernel function $P(\theta|\theta_0)$.

Equations (43)–(45) form the fundamental solutions of the differential equations in (24)–(26). Together with this set of transition probabilities, one can resort to (36), (39), and (38) towards the generic solutions in case of arbitrary initial condition.

3. Long-time behavior of the marginal distributions

Here we investigate the long-term behavior of $P(s_t)$ and $P(\theta_t)$. To do this, looking at (39) and (38), it is enough to consider the limit of the transition kernel functions in (44) and (45) as t tends to infinity. Because the concept of Gaussianity underlies the processes of s and θ , it is natural to make a guess that the long-term probabilistic behavior of the polar variables can be understood in terms of the mean μ' and the variance Σ' , indefinitely evolving according to (35). We demonstrate that this is the case, yet there is some difference between the conditions for $P(s)$ and $P(\theta)$ as clarified below.

As for the amplitude variable, if $\mu' \rightarrow 0$ [equivalently $\Phi_t \rightarrow 0$ in view of (35)] and $\Lambda'_t \rightarrow \bar{\Lambda}$ in growing t , then we have $P(s|s_0) \rightarrow \bar{\Lambda} e^{-\bar{\Lambda}s}$ and the convergence to the exponential distribution occurs. If we have the mean convergence only without the variance convergence, since $I_0(p) \rightarrow 1$ as $p \rightarrow 0$, it is found that $P(s|s_0) \simeq \Lambda'_t e^{-\Lambda'_t s}$ for large t . However, it deserves to note that if there exists $\bar{\Sigma}$ satisfying

$2\gamma\bar{\Sigma} = 2\eta$ (this relation can be met even when γ and η are time dependent) then the mean convergence to zero implies the variance convergence to $\bar{\Sigma}$. This statement is immediately verified from observing that Σ'_t in (35) solves the equation $\dot{\Sigma}' = -2\gamma\Sigma' + 2\eta$, allowing for the relation

$$\Sigma'_t = \bar{\Sigma}(1 - |\Phi_t|^2) \tag{46}$$

so that $\Sigma'_t \rightarrow \bar{\Sigma} = 1/\bar{\Lambda}$ as $t \rightarrow \infty$ and $\mu'_t, \Phi_t \rightarrow 0$. We comment that the limit measure $P(s) = \bar{\Lambda}e^{-\bar{\Lambda}s}$ can be used as the stationary distribution $\varphi_\infty(s)$ for (26).

As for the phase variable, the condition $\mu' \rightarrow 0$ at large times is enough for $P(\theta)$ to converge to the uniform distribution. Since $F(p, q) \rightarrow 1/p$ as $q \rightarrow 0$, the long-time behavior is determined by $P(\theta|s_0, \theta_0) \rightarrow 1/2\pi$. Notice that, unlike the case of amplitude, there is no requirement concerning the variance.

D. Prediction of the true signal

Now we return our attention to the turbulent signal a_k generated from the Hamiltonian system (2).

1. The recipe

Recall that our goal is to estimate the uncertainty in the polar representation of the system variable propagated by the four-wave dynamics of (3). In this regard, our achievement so far can be summarized as follows. For the case when the underlying process a_k is statistically close to the solution of CSM or MSM, one is suggested to approximate the target distribution functions by the probabilities due to the appropriate reduced-order model (in case of the phase variable, the difference between $\theta = \arg(z)$ and $\phi_k = \arg(a_k)$ needs to be cared). This can be accomplished by tuning the adaptive parameters γ and η , associated with CSM and MSM, and applying the prediction mapping (36), (39), and (38) together with the given initial condition and the transition kernels (43)–(45) determined by (35) [and (46) in some cases]. One way to specifying the parameters is via the agreement of the stationary spectrum and decorrelation time of the true and approximate models. For this, the detailed discussion can be found in Ref. [9].

2. Description of weak turbulence using CSM

Here we restrict our discussion to weak turbulence. In this case, it is worth noting that (i) the KFE (25) in connection with CSM is of the same form with the PDE (5) derived from the direct analysis of the true turbulence model and (ii) Eq. (44) is equal to the fundamental solution of the PDE (5) obtained by using the Laplace transform and the method of characteristics in Ref. [2]. From a practical point of view, one is concerned with the accuracy of the approximation of the target distribution function and the emphasis will be placed on the learning scheme for making the parameters γ and η of the approximate model closer to γ_k and η_k of the true model. But the more important consideration is that this agreement between our theoretical prediction by means of CSM and the existing result for weak turbulence not only provides a strong indication that the reduced-order modeling skill is the mathematically reliable tool in arriving at the correct answer

without recourse to possibly very complicated and lengthy calculations which are often indispensable for the treatment of complex dynamical systems but also encourages us to examine MSM and ARM aimed for strong wave turbulence and to demonstrate their plausibility.

Prior to proceeding to discuss other simplified models, however, one should be warned against too much confidence in the ability of a substantial simplification of the complex model in mimicking the genuine dynamical system behavior. The truth is that, even for the weak turbulence, the reality picture shown by the wave turbulent signal is very rich and widely varied so that not all statistics of the turbulence dynamics can be reproduced together with a simpler stochastic differential equation. Incidentally, we numerically demonstrated the validity of the proposed models for the description of the turbulent signal coming from the four-wave dynamical system in thermal equilibrium [8–11]. As for their limitations, providing the relevant discussion in detail is unfortunately beyond the scope of present paper, in which our concern is confined to the situations where the characteristics of the true signal can be captured with reasonable accuracy by the SDE models introduced in Sec. II. Nonetheless, in the sequel, we provide two important remarks on the different implications by the PDE (5) and KFE (25) for the purpose of deepening the understanding of the applicability of the reduced-order model approach for the quantification of uncertainty arising from the wave turbulence.

First, the identical form between the KFE (25) and the PDE (5) must not be interpreted in such a way that the true underlying signal is nearly a Gaussian process. Our argument for this statement is via the random frequency modulation of (17), i.e., the relaxation of the oscillation parameter by adding some random noise. To be precise, we replace γ in the linear model (17) by $\gamma + i\xi$ for some real-valued random process ξ . Note that the resulting process z is clearly very different from Gaussian but the corresponding amplitude process (22) and KFE (25) are unchanged. Note also that in this case, one cannot use the Gaussian function (18) for the derivation of the fundamental solution (44) of the differential equation for the wave amplitude.

Second, the PDE (5) is not the same as but more generic than the KFE (25) due to the varied options for the boundary condition (in addition to the initial condition, boundary conditions have to be specified to uniquely determine the solution of the differential equation which concerns at most the local relationship). The direct consequence is that from the analysis of (5), rather than that of (25), one can extract more information about the weak turbulence system. We verify this point by comparing the two time-independent solutions of the PDE (5):

$$P_k(s) = \frac{1}{\bar{n}_k} \exp\left(-\frac{s}{\bar{n}_k}\right) \tag{47}$$

and

$$\begin{aligned} P_k(s) &= \frac{F}{\eta_k} Ei\left(\frac{s}{\bar{n}_k}\right) \exp\left(-\frac{s}{\bar{n}_k}\right) \\ &\simeq \frac{F}{\gamma_k s} + \frac{\eta_k F}{(\gamma_k s)^2} + \dots \quad \text{when } s \gg \bar{n}_k = \frac{\eta_k}{\gamma_k}, \end{aligned} \tag{48}$$

where F is constant and $Ei(\cdot)$ is integral exponential function. Note the functional form of (47) is equal to that of the unique stationary solution of the KFE (25), which can be obtained by considering the long-term limit of (44). Unlike the exponentially decaying asymptotics of (47) at large amplitudes, the tail behavior of (48) serving as the boundary condition for the PDE (5) is characterized by the algebraic decay and thus any function of the form of (48) cannot be a solution of the KFE (25). In fact, we doubt that the wave turbulence scenario due to (48) can be realized together with stochastic differential equations driven by white noise. Furthermore, we presume that the approximation by means of SDE is apt for the description of the wave turbulent signal in case of statistical equilibrium but not suitable for the steady state of the far-from-equilibrium system for the weak turbulence. This is mainly for the reason that, writing the PDE (5) as the continuity equation $\partial_t P_k = \partial_s \mathcal{F}$ with $\mathcal{F} \equiv 2s(\gamma_k P_k + \eta_k \partial_s P_k)$, Eqs. (47) and (48) are respectively obtained from seeking the solution with the vanishing ($\mathcal{F} = 0$) and the nonzero constant ($\mathcal{F} = F$) probability flux [14,15].

IV. TURBULENT SIGNAL MODELED BY A NON-MARKOV PROCESS

Now let us consider ARM (11). In terms of the variable $z_k(t) = e^{i\Omega_k t} \tilde{a}_k(t)$, the model equation can be rephrased as

$$\begin{aligned} \text{(ARM)} \quad \dot{z} &= -\gamma z + \sqrt{2\eta} \dot{W}_z \\ &\quad - \int_0^t d\tau A e^{-\nu(t-\tau)} z(\tau) + R, \end{aligned} \quad (49)$$

where $R = e^{i\Omega_k t} \tilde{R}$ denotes the OUP. For the prediction of the process z_t in (49), one approach is to analyze this non-Markovian model but the direct treatment of (49) is rather problematic due to the term involving the time integral. We circumvent this difficulty by introducing the bivariate Markov model

$$\begin{aligned} \dot{z} &= Z - \gamma z + \sqrt{2\eta} \dot{W}_z, \\ \dot{Z} &= -\mathcal{A}Z - \nu Z + \sqrt{2\zeta} \dot{W}_Z, \end{aligned} \quad (50)$$

and making use of the fact that the probability of z solving the equation (50) is essentially identical to the distribution of the solution of ARM (49) [10]. Here ζ is the positive parameter in connection with the stationary spectrum of Z , and \dot{W}_Z is complex-valued white noise, independent of \dot{W}_z . Our strategy for estimating the uncertainty of ARM is therefore through analyzing the duet model (50) and performing the marginalization in a suitable manner. Particularly, we determine the joint probability of the couple of variables (z, Z) in Sec. IV A and the marginal distribution of z in Sec. IV B. We discuss how to utilize the resulting knowledge in approximating the probability with reference to the true signal a_k in Sec. IV C.

A. Gaussian process in two dimensions

Note that Eq. (50) is the OUP in two dimensions. Thereby the general discussion of the multivariate OUP, provided in Sec. IV A 1, precedes the case study of (50), provided in Sec. IV A 2.

1. Multivariate Ornstein-Uhlenbeck process

We define a complex-valued Gaussian random vector in d dimensions, denoted by \mathbf{z} , as follows. The real and imaginary parts of each component of \mathbf{z} are independent Gaussians, having the same variance. Let $z = x + iy$ and $Z = X + iY$ be the two different elements of \mathbf{z} . In view of $\langle zZ^* \rangle = xX + yY + i(yX - xY)$, the cross-correlation $\langle zZ^* \rangle = I$ is interpreted as $\langle xX \rangle = \langle yY \rangle = \text{Re}(I)/2$ and $\langle yX \rangle = -\langle xY \rangle = \text{Im}(I)/2$. Here Re means the real part and Im means the imaginary part. Using the notation $\mathbf{z} \sim \mathcal{N}(\boldsymbol{\mu}, \boldsymbol{\Sigma} = \boldsymbol{\Lambda}^{-1})$ (here and after bold is used for indicating vector and matrix), the joint distribution function $P(\{\text{Re}(z_i), \text{Im}(z_i)\}_{i=1}^d)$ for the $2d$ -dimensional real-valued Gaussian vector can be represented as

$$P(\mathbf{z}) = \frac{|\boldsymbol{\Lambda}|}{\pi^d} e^{-(\mathbf{z}-\boldsymbol{\mu})^* \boldsymbol{\Lambda} (\mathbf{z}-\boldsymbol{\mu})}, \quad (51)$$

where modulus means determinant of the matrix and $*$ denotes conjugate transpose.

Let \mathbf{z}_t be governed by the linear system of SDEs

$$d\mathbf{z} = -\mathbf{M}\mathbf{z}dt + \mathbf{L}d\mathbf{W}, \quad (52)$$

where \mathbf{W} denotes a vector of complex-valued mutually independent Brownian motions and the coefficient matrices of \mathbf{M} and \mathbf{L} can be time varying. If the distribution of \mathbf{z}_0 is Gaussian, then the time advance of the mean and covariance of \mathbf{z}_t is determined by

$$\begin{aligned} \dot{\boldsymbol{\mu}} &= -\mathbf{M}\boldsymbol{\mu}, \\ \dot{\boldsymbol{\Sigma}} &= -(\mathbf{M}\boldsymbol{\Sigma} + \boldsymbol{\Sigma}\mathbf{M}^*) + \mathbf{L}\mathbf{L}^*. \end{aligned} \quad (53)$$

Equation (53) can be solved to yield the expressions

$$\begin{aligned} \mathbf{z}_t | \mathbf{z}_0 &\sim \mathcal{N}(\boldsymbol{\mu}'_t, \boldsymbol{\Sigma}'_t = (\boldsymbol{\Lambda}'_t)^{-1}), \\ \boldsymbol{\mu}'_t &= \boldsymbol{\Psi}_t \mathbf{z}_0, \\ \boldsymbol{\Sigma}'_t &= \boldsymbol{\Psi}_t \left(\int_0^t ds \boldsymbol{\Psi}_s^{-1} \mathbf{L}_s \mathbf{L}_s^* (\boldsymbol{\Psi}_s^{-1})^* \right) \boldsymbol{\Psi}_t^*, \end{aligned} \quad (54)$$

and

$$\begin{aligned} \mathbf{z}_t &\sim \mathcal{N}(\boldsymbol{\mu}_t, \boldsymbol{\Sigma}_t = (\boldsymbol{\Lambda}_t)^{-1}), \\ \boldsymbol{\mu}_t &= \boldsymbol{\Psi}_t \boldsymbol{\mu}_0, \\ \boldsymbol{\Sigma}_t &= \boldsymbol{\Psi}_t \boldsymbol{\Sigma}_0 \boldsymbol{\Psi}_t^* + \boldsymbol{\Sigma}'_t, \end{aligned} \quad (55)$$

which are in terms of the matrix $\boldsymbol{\Psi}_t$ satisfying $\dot{\boldsymbol{\Psi}}_t = -\mathbf{M}\boldsymbol{\Psi}_t$ and $\boldsymbol{\Psi}_0$ is the identity matrix.

Suppose there exists a time-independent matrix $\bar{\boldsymbol{\Sigma}}$ such that

$$\mathbf{M}\bar{\boldsymbol{\Sigma}} + \bar{\boldsymbol{\Sigma}}\mathbf{M}^* = \mathbf{L}\mathbf{L}^*, \quad (56)$$

then the relation

$$\boldsymbol{\Sigma}'_t = \bar{\boldsymbol{\Sigma}} - \boldsymbol{\Psi}_t \bar{\boldsymbol{\Sigma}} \boldsymbol{\Psi}_t^* \quad (57)$$

holds. In such case, if $\boldsymbol{\Psi}_t \rightarrow \mathbf{0}$ is satisfied in growing t , then we have the convergence results: $\boldsymbol{\mu}'_t \rightarrow \mathbf{0}$, $\boldsymbol{\Sigma}'_t \rightarrow \bar{\boldsymbol{\Sigma}} = (\bar{\boldsymbol{\Lambda}})^{-1}$, and $P(\mathbf{z} | \mathbf{z}_0) \rightarrow \frac{|\bar{\boldsymbol{\Lambda}}|}{\pi^d} e^{-\mathbf{z}^* \bar{\boldsymbol{\Lambda}} \mathbf{z}}$ as $t \rightarrow \infty$.

2. Case study of the duet model

Here we study the duet model (50) in the rectangular and polar coordinates.

Rectangular coordinate. Note the OUP in (52) reduces to the model equation (50) once the choice of $\mathbf{z} = (z, Z)^T$ and

$$-\mathbf{M} = \begin{pmatrix} -\gamma & 1 \\ -\mathcal{A} & -\nu \end{pmatrix}, \quad \mathbf{L} = \begin{pmatrix} \sqrt{2\eta} & 0 \\ 0 & \sqrt{2\zeta} \end{pmatrix} \quad (58)$$

is made. Here the upper T means transpose. In general, the transition probability

$$P(z, Z|z_0, Z_0) \quad (59)$$

is in the form of the Gaussian function (51) and can be found via replacing $(\boldsymbol{\mu}, \boldsymbol{\Lambda})$ by $(\boldsymbol{\mu}', \boldsymbol{\Lambda}')$ in (54).

Let us consider the particular situation where the coefficients in (50) are constants. Then the matrix exponential $\boldsymbol{\Psi}_t$ is given by

$$\begin{aligned} \boldsymbol{\Psi}_t &= \exp(-\mathbf{M}t) \\ &= e^{-\frac{\gamma+\nu}{2}t} \\ &\times \begin{bmatrix} \cos\left(\frac{\mathcal{R}t}{2}\right) - \frac{\gamma-\nu}{\mathcal{R}} \sin\left(\frac{\mathcal{R}t}{2}\right) & \frac{2}{\mathcal{R}} \sin\left(\frac{\mathcal{R}t}{2}\right) \\ -\frac{2\mathcal{A}}{\mathcal{R}} \sin\left(\frac{\mathcal{R}t}{2}\right) & \cos\left(\frac{\mathcal{R}t}{2}\right) + \frac{\gamma-\nu}{\mathcal{R}} \sin\left(\frac{\mathcal{R}t}{2}\right) \end{bmatrix}, \end{aligned} \quad (60)$$

where $\mathcal{R} = \sqrt{4\mathcal{A} - (\gamma - \nu)^2}$. Furthermore, if the conditions $\bar{n} = \eta/\gamma$ and $\bar{N} = \zeta/\nu_r = \mathcal{A}\bar{n}$ are fulfilled, then the matrix

$$\bar{\boldsymbol{\Sigma}} = \text{diag}(\bar{n}, \bar{N}) \quad (61)$$

is the solution of (56). In this case, one can make use of (57), (60), and (61) to compute $\boldsymbol{\Sigma}'$ in (54) with ease.

Polar coordinate. Let $z = \sqrt{s}e^{i\theta}$, $Z = \sqrt{S}e^{i\Theta}$, and let $\vartheta = \theta - \Theta$ be the phase difference. The polar components of the variables in (50) are governed by the Itô differential equations

$$\begin{aligned} ds &= [2\eta - 2\gamma s + 2\sqrt{sS} \cos(\vartheta)]dt + \sqrt{4\eta s} dB_s, \\ d\theta &= \left(-\frac{1}{s}\right)\sqrt{sS} \sin(\vartheta)dt - \sqrt{\frac{\eta}{s}} dB_\theta, \\ dS &= [2\zeta - 2\nu_r S - 2\mathcal{A}\sqrt{sS} \cos(\vartheta)]dt + \sqrt{4\zeta S} dB_S, \\ d\Theta &= \left[\left(-\frac{\mathcal{A}}{S}\right)\sqrt{sS} \sin(\vartheta) - \nu_i\right]dt - \sqrt{\frac{\zeta}{S}} dB_\Theta, \end{aligned} \quad (62)$$

and the KFE corresponding to (62) reads

$$\begin{aligned} \partial_t P(t, s, \theta, S, \Theta) &= \partial_s [2\gamma s P + 2\eta s \partial_s P - 2\sqrt{sS} \cos(\vartheta) P] \\ &+ \partial_\theta \left[\frac{1}{s} \sqrt{sS} \sin(\vartheta) P + \frac{\eta}{2s} \partial_\theta P \right] \\ &+ \partial_S [2\nu_r S P + 2\zeta S \partial_S P + 2\mathcal{A}\sqrt{sS} \cos(\vartheta) P] \\ &+ \partial_\Theta \left[\frac{\mathcal{A}}{S} \sqrt{sS} \sin(\vartheta) P + \nu_i P + \frac{\zeta}{2S} \partial_\Theta P \right]. \end{aligned} \quad (63)$$

The fundamental solution of (63) is given by the transition probability

$$P(s, \theta, S, \Theta|s_0, \theta_0, S_0, \Theta_0) \quad (64)$$

and can be obtained by applying the change of variables to the Gaussian function of (59) and multiplying the Jacobian $\mathcal{J} = (1/2)^2$ as a consequence of the coordinate transformation from (z, Z) to (s, θ, S, Θ) .

In line with the discussion in Sec. III B 3, the SDEs governing $|z| = \rho$ and $|Z| = \mathcal{P}$ read

$$\begin{aligned} d\rho &= \left[\frac{\eta}{2\rho} - \gamma\rho + \mathcal{P} \cos(\vartheta) \right] dt + \sqrt{\eta} dB_\rho, \\ d\mathcal{P} &= \left[\frac{\zeta}{2\mathcal{P}} - \nu_r \mathcal{P} - \mathcal{A}\rho \cos(\vartheta) \right] dt + \sqrt{\zeta} dB_\mathcal{P} \end{aligned} \quad (65)$$

and can be used instead of the equations for s and S in (62). The counterpart of (64) in terms of the set of variables $(\rho, \theta, \mathcal{P}, \Theta)$ can be obtained by making the change of variables in (59) and taking care of the Jacobian $\mathcal{J} = \rho\mathcal{P}$.

B. Marginalized process

Now we concentrate on the processes of z , $s = |z|^2$, $\theta = \arg(z)$ among the variables in (50) and (62) and study their time-evolving probability distributions. In view of (50), the information of $P(z_0)$ is not sufficient and we need to know $P(z_0, Z_0)$ in order to completely determine $P(z_t)$ [and $P(s_t, \theta_t)$]. Below, we will discuss the three cases in decreasing order of generality: (i) $P(z_0, Z_0)$ is arbitrary (Sec. IV B 1), (ii) $P(Z_0|z_0)$ is Gaussian (Sec. IV B 2), and (iii) $P(z_0, Z_0)$ is jointly Gaussian (Sec. IV B 3). We investigate the long-time behavior of the probability of s and θ in Sec. IV B 4.

1. The case of arbitrary $P(z_0, Z_0)$

The mapping from $P(z_0, Z_0)$ to $P(z_t)$ can be achieved through the integral

$$P(z) = \int dz_0 dZ_0 P(z|z_0, Z_0) P(z_0, Z_0). \quad (66)$$

Note the law of the process $z_t|z_0, Z_0$ is found by averaging out the variable Z from the joint Gaussian of (54) with $\mathbf{z} = (z, Z)^T$ and given by

$$\begin{aligned} z_t|z_0, Z_0 &\sim \mathcal{N}(\boldsymbol{\mu}'_{t,z}, \boldsymbol{\Sigma}'_{t,zz}), \\ \boldsymbol{\mu}'_{t,z} &= \mathbf{e}_1^T \boldsymbol{\mu}'_t = \boldsymbol{\Psi}_{t,11} z_0 + \boldsymbol{\Psi}_{t,12} Z_0, \\ \boldsymbol{\Sigma}'_{t,zz} &= \mathbf{e}_1^T \boldsymbol{\Sigma}'_t \mathbf{e}_1, \end{aligned} \quad (67)$$

where \mathbf{e}_1 is column vector with the first element 1 and zero otherwise. The conditional probability $P(z|z_0, Z_0)$ takes the form of Gaussian function (18) where the mean and variance are given by the ones in (67).

The counterpart of (66) in terms of the polar variables reads as

$$\begin{aligned} P(s, \theta) &= \int ds_0 d\theta_0 dS_0 d\Theta_0 P(s, \theta|s_0, \theta_0, S_0, \Theta_0) \\ &\times P(s_0, \theta_0, S_0, \Theta_0) \end{aligned} \quad (68)$$

and allows us to perform the mapping from $P(s_0, \theta_0, S_0, \Theta_0)$ to $P(s_t, \theta_t)$ [and to $P(s_t)$ and $P(\theta_t)$ after the integration of (68) over the irrelevant variable]. The conditional probabilities $P(s, \theta|s_0, \theta_0, S_0, \Theta_0)$, $P(s|s_0, \theta_0, S_0, \Theta_0)$, and $P(\theta|s_0, \theta_0, S_0, \Theta_0)$ are obtained by applying the machinery developed in Secs. III C 1 and III C 2 to the Gaussian process

of (67), and given by the form of (27), (28), and (30), with replacing (μ, Σ) by $(\mu'_{t,z}, \Sigma'_{t,zz})$ in (67).

The above-mentioned conditional probabilities are the fundamental solutions of the differential equations determining the evolution of the corresponding marginal distribution functions. As in Sec. III B 1, the governing equations can be derived from performing the projection of the KFE (63) onto the space of some of the entire variables. For instance, the integrodifferential equation for $P(t, s, \theta) = \int dS d\Theta P(t, s, \theta, S, \Theta)$ takes the same form as (26), provided that the forward operator $L = L_0 + L_1$ with

$$L_0 = \partial_S [2\nu_r S + 2\xi S \partial_S] + \partial_\Theta \left[\frac{\xi}{2S} \partial_\Theta \right],$$

$$L_1 = \partial_s [2\gamma s + 2\eta s \partial_s - 2\sqrt{sS} \cos \vartheta] + \partial_S [2A\sqrt{sS} \cos \vartheta]$$

$$+ \partial_\theta \left[\frac{1}{s} \sqrt{sS} \sin \vartheta + \frac{\eta}{2s} \partial_\theta \right] + \partial_\Theta \left[\frac{A}{S} \sqrt{sS} \sin \vartheta + \nu_i P \right],$$
(69)

and the projection operator \mathcal{P} defined as $\mathcal{P}f(s, \theta, S, \Theta) = \varphi_\infty(S, \Theta) \int dS d\Theta f(s, \theta, S, \Theta)$ are used. For the case of the constant coefficients in the duet model (50), which we considered at the end of Sec. IV A 2 a, since the stationary distribution is given by $P(s, S, \theta, \Theta) = (\frac{1}{2\pi})^2 \times \frac{1}{\tilde{n}} e^{-\frac{s}{\tilde{n}}} \times \frac{1}{\tilde{N}} e^{-\frac{\Theta}{\tilde{N}}}$, the invariant measure $P(S, \Theta) = \frac{1}{2\pi} \frac{1}{\tilde{N}} e^{-\frac{\Theta}{\tilde{N}}}$ can be used as $\varphi_\infty(S, \Theta)$.

2. The case when $P(Z_0|z_0)$ is Gaussian

One can get rid of the appearance of Z_0 in (66) and formulate the direct mapping from $P(z_0)$ to $P(z_t)$. This can be achieved by converting (66) into (34) with the help of

$$P(z|z_0) = \int dZ_0 P(z|z_0, Z_0) P(Z_0|z_0). \quad (70)$$

It is worth noting that when $Z_0|z_0$ is Gaussian, the integration in (70) is analytically tractable and the resulting process $z_t|z_0$ is also Gaussian. In particular, let $P(Z_0|z_0) = \mathcal{N}(\mu_{Z_0|z_0}, \Sigma_{Z_0|z_0})$ then the conditioned law of $z_t|z_0$ is given by

$$z_t|z_0 \sim \mathcal{N}(\mu''_t, \Sigma''_t = 1/\Lambda''_t),$$

$$\mu''_t = \Psi_{11} z_0 + \Psi_{12} \mu_{Z_0|z_0}, \quad (71)$$

$$\Sigma''_t = \Sigma'_{11} + |\Psi_{12}|^2 \Sigma_{Z_0|z_0},$$

where double prime is used in order to distinguish from the formula (35) for the univariate OUP (17). Equation (71) is obtained from plugging in $\mu'_z = \Psi_{11} z_0 + \Psi_{12} \mu_{Z_0|z_0}$ into $(\Sigma'_{z_0|z_0})^{-1} |Z_0 - \mu_{Z_0|z_0}|^2 + (\Sigma'_{zz})^{-1} |z - \mu'_z|^2$ and using the identity $A|z - a|^2 + B|z - b|^2 = (A + B)|z - \frac{Aa + Bb}{A+B}|^2 + \frac{AB}{A+B} |a - b|^2$ where $A, B > 0$ and $z, a, b \in \mathbb{C}$.

As was done in Sec. III C 2, the transition probabilities for the polar variables are inherited from the Gaussian function of the rectangular form and given by

$$P(s, \theta|s_0, \theta_0) = \frac{\Lambda''}{2\pi} e^{-\Lambda''(s+|\mu''|^2 - 2\sqrt{s}|\mu''| \cos[\theta - \arg(\mu'')])}, \quad (72)$$

$$P(s|s_0, \theta_0) = \Lambda'' e^{-\Lambda''(s+|\mu''|^2)} I_0(2\Lambda'' \sqrt{s} |\mu''|), \quad (73)$$

$$P(\theta|s_0, \theta_0) = \frac{\Lambda''}{2\pi} e^{-\Lambda''|\mu''|^2} F(\Lambda'', |\mu''| \cos[\theta - \arg(\mu'')]), \quad (74)$$

for which (71) is used. In comparison to (44), the attention is drawn to the presence of θ_0 in (73). Given the initial condition $P(s_0, \theta_0)$, one can obtain the expressions for $P(s|s_0)$ and $P(\theta|s_0)$ by applying (73) and (74) to (41) and (42).

Note that the variables s_0 and θ_0 are implicitly involved in (72)–(74) through μ''_t and Σ''_t in (71). It is instructive to illustrate the case when the dependency is explicitly visible. In particular, let us consider the situation where (i) $\mu_{Z_0|z_0}$ is a linear function of z_0 , and (ii) $\Sigma_{Z_0|z_0}$ does not depend on z_0 , so that the emergence of s_0 and θ_0 is through μ''_t only and not through $\Sigma''_t = 1/\Lambda''_t$. In such a case, we can write μ''_t in (71) as

$$\mu''_t = \Phi'_t z_0 + \Phi'_t, \quad (75)$$

and the dependence of (72)–(74) on s_0 and θ_0 can be seen from

$$|\mu''|^2 = s_0 |\Phi'_t|^2 + |\Phi'_t|^2$$

$$+ 2\sqrt{s_0} |\Phi'_t| |\Phi'_t| \cos[\theta_0 + \arg(\Phi'_0) - \arg(\Phi'_t)],$$

$$\arg(\mu'') = \arg(\Phi'_t \sqrt{s_0} e^{i\theta_0} + \Phi'_t). \quad (76)$$

In view of (44), a natural question of when $P(s|s_0, \theta_0)$ in (73) reduces to $P(s|s_0)$ arises. Evidently this occurs when $\Phi'' = 0$ [otherwise, $P(s|s_0, \theta_0)$ depends on θ_0], and the desired formula for $P(s|s_0)$ can be obtained via replacing the two parameters (Φ, Λ') that appear at (44) by (Φ', Λ'') in (75) and (71).

3. The case when $P(z_0, Z_0)$ is Gaussian

In cases where $P(z_0, Z_0) = \mathcal{N}(\mu_0, \Sigma_0 = (\Lambda_0)^{-1})$ is jointly Gaussian, the conditioned variable $Z_0|z_0$ is also Gaussian and the law is given by

$$Z_0|z_0 \sim \mathcal{N}(\mu_{Z_0|z_0}, \Sigma_{Z_0|z_0}),$$

$$\mu_{Z_0|z_0} = \mu_{0,Z} + \Sigma_{0,Zz} \Sigma_{0,zz}^{-1} (z_0 - \mu_{0,z}),$$

$$\Sigma_{Z_0|z_0} = \Sigma_{0,ZZ} - \Sigma_{0,Zz} \Sigma_{0,zz}^{-1} \Sigma_{0,zZ}. \quad (77)$$

Equation (77) is one specific example of the circumstances we assumed in the preceding paragraph, i.e., Eq. (75) is satisfied alongside

$$\Phi' = \Psi_{11} + \Psi_{12} \Sigma_{0,Zz} \Sigma_{0,zz}^{-1},$$

$$\Phi'' = -\Psi_{12} \Sigma_{0,Zz} \Sigma_{0,zz}^{-1} \mu_{0,z} + \Psi_{12} \mu_{0,Z}. \quad (78)$$

Recall the variable θ_0 in (73) can be eliminated if Φ'' vanishes and this is the case, for instance, when $\mu_{0,z} = \mu_{0,Z} = 0$.

4. Long-time behavior of the marginal distributions

In general, we can figure out the long-term behavior of $P(s_t)$ and $P(\theta_t)$ from considering the proper marginalization of (68) in the limit of $t \rightarrow \infty$. In order to obtain this knowledge, it suffices to study the long-time behavior of the transition kernels, determined by the mean and variance in (67).

As for the amplitude variable, both of the conditions for the mean $\mu'_{t,z} \rightarrow 0$ and the variance $\Sigma'_{t,zz} \rightarrow \bar{\Sigma}_{zz}$ are needed for the convergence $P(s|s_0, \theta_0, S_0, \Theta_0) \rightarrow e^{-s/\bar{\Sigma}_{zz}} / \bar{\Sigma}_{zz}$ to the

exponential distribution in the growth of t . Note this holds in the specific case under consideration in Sec. IV A 2 a.

As for the phase variable, in view of (67), the sufficient condition for the convergence $P(\theta|s_0, \theta_0, S_0, \Theta_0) \rightarrow 1/2\pi$ to the uniform distribution over the circle is that the mean $\mu'_{t,z}$ goes to zero as $t \rightarrow \infty$.

C. Prediction of the true signal

Suppose that the true signal a_k resulting from the four-wave system and the solution of ARM are statistically similar to each another. Then one can make use of the analysis of ARM performed in the preceding sections to estimate the propagating probability of a_k . In view of (16a) and (49), the variable Z in (50) is a statistical approximation of $e^{i\Omega_k t} A_k$. This implies that for the case when the auxiliary variable A_k in (15b) behaves like Gaussian (we believe this presumption is legitimate in many cases due to the collective effect of chaotic interactions, which is a manifestation of the central limit theorem), the recipe is that (i) one trains ARM, for example, via the agreement between the autocorrelation functions by the true signal and ARM [11], and (ii) one exploits the transition probabilities (72)–(74) determined by Eqs. (57), (60), (61), and (71) together with the rules (36)–(38) in order to approximately quantify the uncertainty as to the polar representation of a_k .

V. NUMERICAL SIMULATIONS

Here we numerically demonstrate that ARM is superior to MSM in describing some statistical properties of the short-wave turbulent signal generated from the four-wave system with strong nonlinearity. The discrepancy between the predictions by MSM and ARM will be highlighted in both cases of the stationary distribution (Sec. V A) and of the irreversible relaxation to the steady state (Sec. V B) for the single wave-profile a_k .

A. Equilibrium state

Our presentation is in the context of the generalized Majda-McLaughlin-Tabak (MMT) system, which is the representative example of the turbulence model (2) and (3) determined by $\omega_k = |\hat{k}|^\alpha$ and $W_{3k}^{12} = |\hat{k}_1 \hat{k}_2 \hat{k}_3 \hat{k}|^{\frac{\beta}{4}}$, where $\hat{k} \equiv k\pi/N$ and N is total number of Fourier modes [9,12,16,17]. Here α and β are the positive parameters, controlling the linear dispersion relation and the strength of the four-wave interactions. Let us consider two instances of the strongly nonlinear system in possession of the set of parameters: (i) $\chi = 1$, $\alpha = 1/2$, $\beta = 3$, $C_\beta = 3/10$ and (ii) $\chi = 0$, $\beta = 1$, $C_\beta = 9/10$, where $C_\beta = 2 \sum_k |\hat{k}|^{\frac{\beta}{2}} \langle |a_k|^2 \rangle$. In both cases, we choose the domain size $N = 512$ so that k ranges as $|k| \leq N/2 = 256$ and simulate the dynamics for sufficiently long time so that the system reaches the thermal equilibrium state characterized by the stationary spectrum

$$\langle |a_k|^2 \rangle = \frac{T}{|\hat{k}|^\alpha + C_\beta |\hat{k}|^{\frac{\beta}{2}}}, \quad (79)$$

where T is the temperature. The details of the direct numerical simulation setting are described in Refs. [9,16,17].

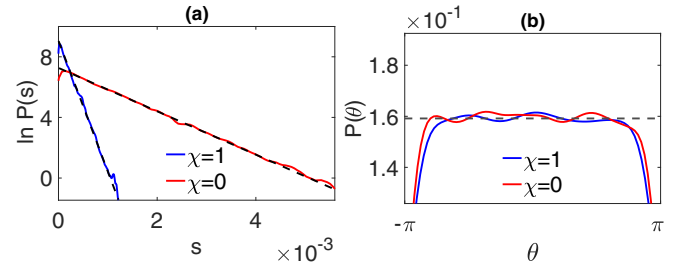


FIG. 1. The solid lines are the stationary distributions $P(s_k)$ and $P(\theta_k)$ for the MMT signal a_k with $k = 192$. The dashed lines are the exponential distribution for the amplitude variable (left) and the uniform distribution for the phase variable (right).

This simulation of the MMT model allows us to produce an individual trajectory of the turbulent signal and we take the shortwave a_k with the high wave number $k = 192$ as the target system variable generating the true signal. These sequential data in time are used to create Fig. 1 and Fig. 2. In Fig. 1, we depict the stationary distributions for the polar variables. The predictions by MSM and ARM are in good agreement with the numerically measured ones from the MMT signal. In Fig. 2, we depict the time correlation functions for the canonical variable in rectangular coordinate. The comparison analysis reveals that ARM outperforms MSM; while the exponential function predicted by MSM is unable to reproduce the more complicated autocorrelation function indicated by the MMT signal, the prediction by ARM, which is given by the first component of (60) up to constant multiplication, can fully recover the numerically found correlation function with high accuracy.

B. Relaxation to equilibrium

Turning our attention to the conditional probability distribution, we draw a number of random samples from $P(a_k(t)|a_k(0))$ at fixed time t in the following way. We first pick up one set of a_k for all k as the realization of the MMT trajectories in equilibrium and replace the value of a_k for fixed $k = 192$ by a particular number for the purpose of making the initial condition $a_k(0)$ as the Dirac Delta function. We next apply the forward solver of the full wave system in equilibrium to find $a_k(t)$ and take it as one sample from

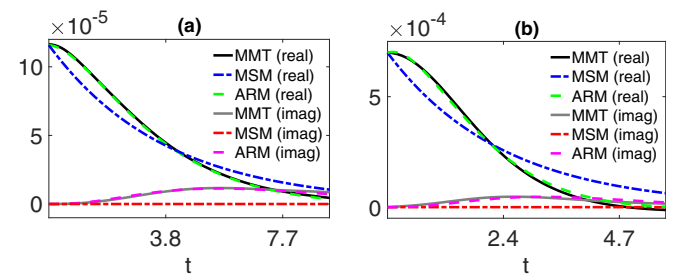


FIG. 2. The two-point function $\langle b_k(t)b_k^*(0) \rangle$ for the MMT signal $b_k = e^{i\Omega_k t} a_k$ with $k = 192$ is depicted as the function of t . The prediction by MSM is $\langle z_t z_0^* \rangle = \bar{n}_k \exp(-t/T_c)$, where \bar{n}_k is the stationary spectrum and T_c is the decorrelation time of the MMT signal. Left: $\chi = 1$; right: $\chi = 0$.

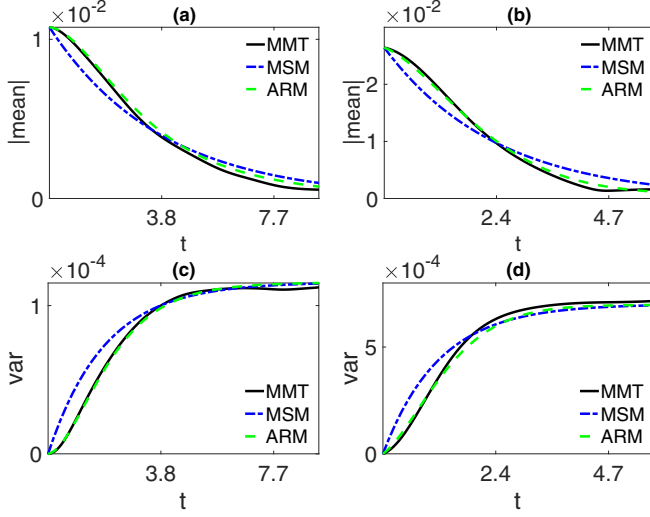


FIG. 3. The solid lines correspond to $|E(a_k(t)|a_k(0))|$ (top) and $\text{Var}(a_k(t)|a_k(0))$ (bottom) of the MMT signal with $k = 192$ as the function of t . The quantities are calculated using the samples of size $2^{12} = 4096$, and the given variable is set to $a_k(0) = \sqrt{\bar{n}_k} e^{i\pi/4}$. The predictions $|\mu'_t|$ and Σ'_t by MSM and ARM are shown for comparison purposes. Left: $\chi = 1$; right: $\chi = 0$.

$P(a_k(t)|a_k(0))$. This set of Monte Carlo samples forward in time is obtained to simulate the decay process to the stationary distribution.

Figure 3 shows the evolution of the mean and variance of $a_k(t)$, calculated using the ensemble average; the predictions by MSM and by ARM, i.e., Eqs. (35) and (71) are also depicted. Figure 4 and Fig. 5 show the distribution functions of the amplitude and phase for a number of fixed times; the transition probabilities (44) and (45) for MSM and (73) and (74) for ARM are also depicted. The comparison analysis in these plots supports our demonstration that ARM is more accurate than MSM in estimating the probability of the MMT signal.

VI. CONCLUDING REMARKS

In this work we apply the reduced-order model approach for the analysis of the evolving probability of the wave magnitude and the phase angle of the canonical variable solving the nonlinear Hamiltonian system characterized by the four-wave interactions. Note that our approach is not through a straightforward analysis of the underlying turbulence model but is inspired and guided by the statistical-mechanical treatment of complex physical models comprising an enormously large number of degrees of freedom. We adopt this way of accessing the problem for the reason that, in contrast to the case of weak turbulence where one can derive the PDE (5) by exploiting the smallness of H_4/H_2 and performing the perturbative analysis, the loss of this apparent small parameter in case of strong nonlinearity prevent us from applying the regular perturbation method for the analysis of the turbulence system driven by strong wave-wave interactions.

We remark that despite a variety of simplified stochastic models, including both Markovian and non-Markovian ones, which we adopted in this work to handle the turbulent

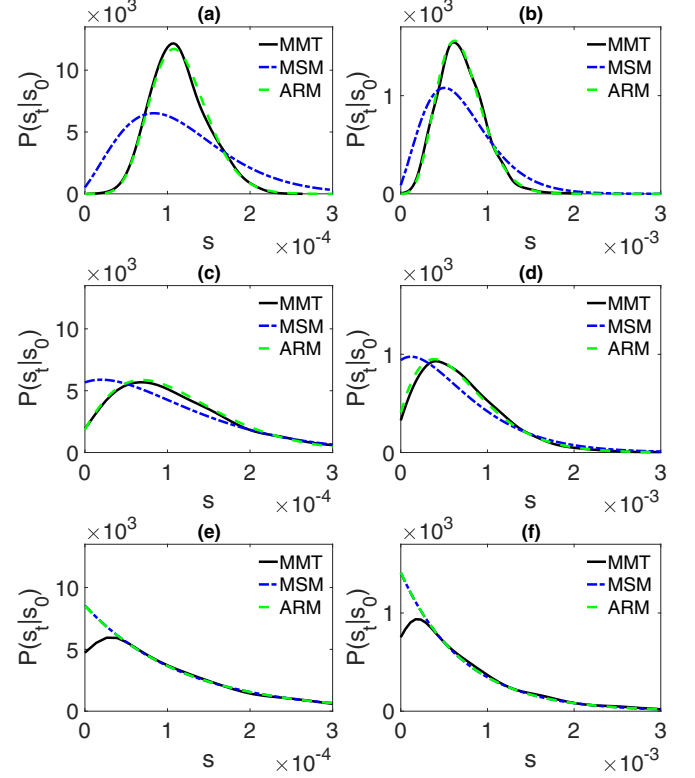


FIG. 4. For the dynamics discussed in Fig. 3, the probabilities of $P(s_t|s_0)$ for $t = r \times T_c$ with $r = 0.1$ (top), $r = 0.3$ (middle), and $r = 1$ (bottom) are presented. Left: $\chi = 1$; right: $\chi = 0$.

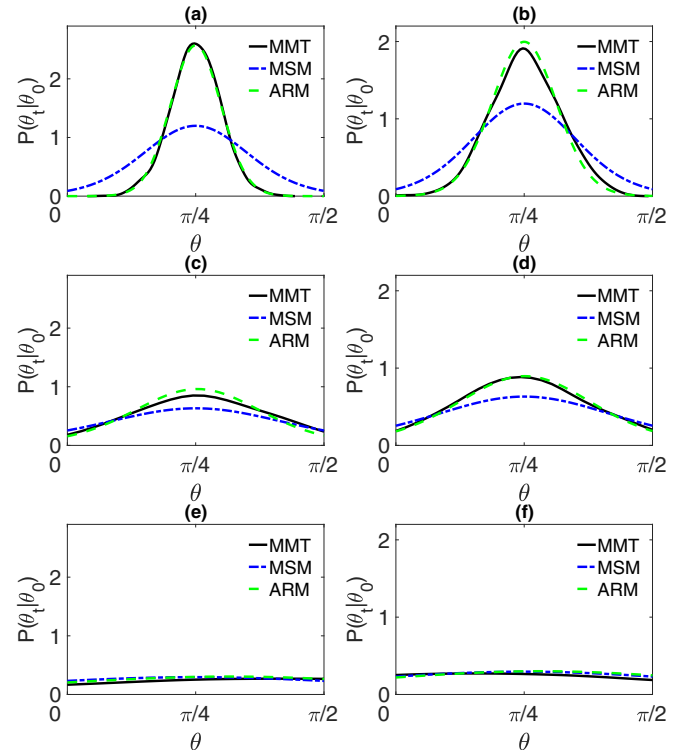


FIG. 5. For the dynamics discussed in Fig. 3, the probabilities of $P(\theta_t|\theta_0)$ for $t = r \times T_c$ with $r = 0.1$ (top), $r = 0.3$ (middle), and $r = 1$ (bottom) are presented. Left: $\chi = 1$; right: $\chi = 0$.

dynamics ranging from weakly to strongly interacting nonlinear waves, the common thing underpinning in all models is the Gaussianity of the process. Performing the numerical study in the context of the Majda-McLaughlin-Tabak model and being assured of the feasibility of our methodology in the case of the complex dynamical system in equilibrium, we plan to pursue the research of addressing the turbulence dynamics in nonequilibrium steady state and to take a further step towards the radical extension of the applicability of the SDE-based approach for the analysis of turbulent signals. The solution scenario in the case of near equilibrium is presumably not much different from the equilibrium case, i.e., Gaussian process modeling remains to be an effective tool. However, in approximating the random signal generated from the complex system whose deviation from the equilibrium state is notably significant, we anticipate a poor performance of the linear models. One reason for this is that the validity regime of linear dynamical systems is restricted to linear transport laws for averaged variables so that they are inevitably inadequate to

the treatment of nonlinear transport processes. Due to this possibly limited applicability of Gaussian process models, the subsequent endeavor will be directed towards developing nonlinear and non-Gaussian models and examining their performances for complex dynamical systems out of equilibrium.

ACKNOWLEDGMENTS

The author thanks Yeontaek Choi and Sergey Nazarenko for useful discussions. The author also thanks the anonymous referees for their helpful comments and suggestions, which indeed contributed to improving the quality of the publication. This work is supported by the Start-up Research Grant of Beijing Normal University (Grant No. 28704-310432107), the United International College Start-up Research Fund (Grant No. UICR0700040-22), and the National Natural Science Fund of China (NSFC) Research Fund for International Excellent Young Scientists (Grant No. 12250610190).

-
- [1] T. Bohr, M. Jensen, G. Paladin, and A. Vulpiani, *Dynamical Systems Approach to Turbulence* (Cambridge University Press, Cambridge, UK, 2005), Vol. 8.
 - [2] S. Nazarenko, *Wave Turbulence* (Springer Science & Business Media, New York, 2011), Vol. 825.
 - [3] V. E. Zakharov, V. S. L'vov, and G. Falkovich, *Kolmogorov Spectra of Turbulence I: Wave Turbulence* (Springer Science & Business Media, New York, 2012).
 - [4] V. Yakhot and V. Zakharov, *Physica D* **64**, 379 (1993).
 - [5] Y. Choi, Y. V. Lvov, S. Nazarenko, and B. Pokorni, *Phys. Lett. A* **339**, 361 (2005).
 - [6] Y. Choi, Y. V. Lvov, and S. Nazarenko, *Physica D* **201**, 121 (2005).
 - [7] Y. Choi, S. Jo, Y.-S. Kwon, and S. Nazarenko, *J. Phys. A: Math. Theor.* **50**, 355502 (2017).
 - [8] W. Lee, *Phys. Rev. E* **98**, 022137 (2018).
 - [9] W. Lee, *J. Nonlinear Sci.* **29**, 1865 (2019).
 - [10] W. Lee, *Phys. Rev. E* **103**, 052101 (2021).
 - [11] W. Lee, *Commun. Math. Sci.* (to be published).
 - [12] W. Lee, G. Kovačič, and D. Cai, *Proc. Natl. Acad. Sci. USA* **110**, 3237 (2013).
 - [13] R. Kubo, M. Toda, and N. Hashitsume, *Statistical Physics: Nonequilibrium Statistical Mechanics* (Springer, Berlin, 1992), Vol. 2.
 - [14] Y. V. Lvov, S. Nazarenko, and B. Pokorni, *Physica D* **218**, 24 (2006).
 - [15] P. Denissenko, S. Lukaschuk, and S. Nazarenko, *Phys. Rev. Lett.* **99**, 014501 (2007).
 - [16] A. J. Majda, D. McLaughlin, and E. Tabak, *J. Nonlin. Sci.* **7**, 9 (1997).
 - [17] W. Lee, G. Kovačič, and D. Cai, *Phys. Rev. Lett.* **103**, 024502 (2009).